An Intriguing Co-Existence: Atrial Myxoma and Cerebral Cavernous Malformations: Case Report and Review of Literature

Shikha Sharma, MD, Daniel Tsyvine, MD, Pierre D. Maldjian, MD, Justin T. Sambol, MD, Constantinos J. Lovoulos, MD, Gal Levy, MD, Amin Maghari, MD, Marc Klapholz, MD, and Muhamed Saric, MD, PhD, *Newark, New Jersey*

It is commonly postulated that neurologic complications of atrial myxomas are due to either direct tumor embolization or mycotic aneurysm of cerebral vasculature or rupture of mycotic aneurysms of cerebral arteries. However, the authors report the case of 63-year-old woman with a large left atrial myxoma whose progressive left-sided weakness was due to a different neurologic mechanism, namely, multiple bleeding cavernous malformations, which were visualized by magnetic resonance imaging of the brain. Cerebral cavernous malformations coexist with mesenchymal anomalies of other organs, including the liver, kidneys, and retinas. To the best of the authors' knowledge, this is only the second reported case of coexistent cerebral cavernous malformations and atrial myxoma. (J Am Soc Echocardiogr 2010;■:■-■.)

Keywords: Echocardiography, Benign cardiac tumor, Left atrium, Myxoma, Cavernous malformations

CASE PRESENTATION

A 63-year-old Costa Rican woman with a history of systemic hypertension was hospitalized after developing progressive left-sided weakness, headache, and dizziness over the preceding 2 months. She experienced neither seizures nor loss of consciousness. There was no weight loss, fever, cough, shortness of breath, or chest pain. She used no illicit drugs or over-the-counter products. Her family history was unremarkable. Written informed consent was obtained from the patient for the publication of this case and accompanying images.

On admission, the patient had a regular heart rate of 70 beats/min, blood pressure of 150/70 mm Hg, an oral temperature of 98.5°F, and room-air oxygen saturation of 99%. On physical exam, her lungs were clear to auscultation bilaterally. A cardiac exam revealed normal-intensity first and second heart sounds and a grade 2/6 rumbling diastolic murmur best heard at the apex. A low-intensity sound was heard at the left lower sternal border with each diastole, consistent with tumor plop. There was no peripheral edema. Neurologic examination revealed loss of muscle strength (4 on a scale of 5) and decreased deep tendon reflexes in both the left arm and the left leg.

Complete blood count, coagulation panel, and blood chemistry were unremarkable, including normal serum troponin I and brain natriuretic peptide levels. Liver, kidney, and thyroid function test results were also within normal limits. Electrocardiographic results were normal. Chest x-ray revealed a normal-sized heart with no pulmonary venous congestion.

Computed tomography of the head on presentation revealed lesions in the right parietal and left occipital lobes, with mixed areas of high and low density, consistent with hemorrhage within the lesions and extensive vasogenic edema in the surrounding areas. The patient was started on phenytoin and intravenous steroids. Subsequent magnetic resonance imaging of the head delineated lesions as multiple bleeding cavernous hemangiomas with surrounding edema and mild midline shift (Figure 1).

Transthoracic echocardiography revealed a large heterogeneous multilobulated mass in the left atrium measuring ≥5.6 × 2.7 cm. The mass was adherent to the interatrial septum and glided over the atrial side of the anterior mitral leaflet (Figure 2, Video 1). It prolapsed into the mitral valve orifice during diastole (tumor plop), causing mild mitral valve stenosis with a mean gradient of 4 mm Hg at a heart rate of 65 beats/min. After intravenous injection of perflutren lipid microsphere contrast (Definity; Lantheus Medical Imaging, North Billerica, MA), there was a heterogenous uptake pattern within the mass. All these findings were pathognomonic for left atrial myxoma (Video 2).

Subsequently, cardiac magnetic resonance imaging was performed using balanced cine gradient-echo sequence (fast imaging employing steady-state acquisition), nonbalanced cine gradient-echo sequence (FASTCINE, GE Healthcare, Milwaukee, WI), and contrast enhancement protocols. The mass exhibited high signal intensity on the T1-weighted and T2-weighted images. No fat was demonstrated within the mass on fat saturation images. On the bright-blood sequences, the mass was not visible on the balanced gradient-echo sequences but could be seen on the nonbalanced bright-blood sequences. After the administration of contrast, enhancement was present at the periphery of the mass. The bright-blood images demonstrated a complete return of the mass into the left atrial cavity in systole and prolapse through the mitral valve into the left ventricle during diastole. There was also suggestion on the bright-blood images that the mass was attached to the interatrial septum via a stalk. On the four-

From the Departments of Medicine (S.S., D.T., M.K., M.S.), Radiology (P.D.M.), Surgery (J.T.S., K.L., G.L.), and Pathology (A.M.), New Jersey Medical School, Newark, New Jersey.

Reprint requests: Muhamed Saric, MD, PhD, New York University, Division of Cardiovascular Diseases, 560 First Avenue, New York, NY 10016 (E-mail: *muhamed.saric@nyumc.org*).

0894-7317/$36.00

doi:10.1016/j.echo.2010.06.009

Abbreviations
CCM = Cerebral cavernous malformations

chamber fast imaging employing steady-state acquisition sequences, there was turbulent flow across the mitral valve during diastole indicative of mitral stenosis). All magnetic resonance imaging findings were consistent with left atrial myxoma (Figure 3, Video 3). Cerebral angiography did not demonstrate aneurysms of any intracerebral vessel.

During the hospital course, the patient's neurologic deficits resolved within a week. She then underwent surgical resection of the left atrial mass without complications (Figure 4). Surgical pathology revealed scattered stellate cells or myxoma cells in abundant matrix with poorly formed vessels. On immunohistochemistry, the lesion was positive for myxoma markers, namely cluster of differentiation 34 and calretinin.

DISCUSSION

In 1952, Goldberg *et al.*[1] reported the first antemortem diagnosis of atrial myxoma by angiocardiography in a 3-year-old child with recurrent right hemiparesis. Neurologic manifestations have been reported in 25% to 45% of cases of atrial myxomas.[2] It is commonly postulated that neurologic complications of atrial myxomas are due to either

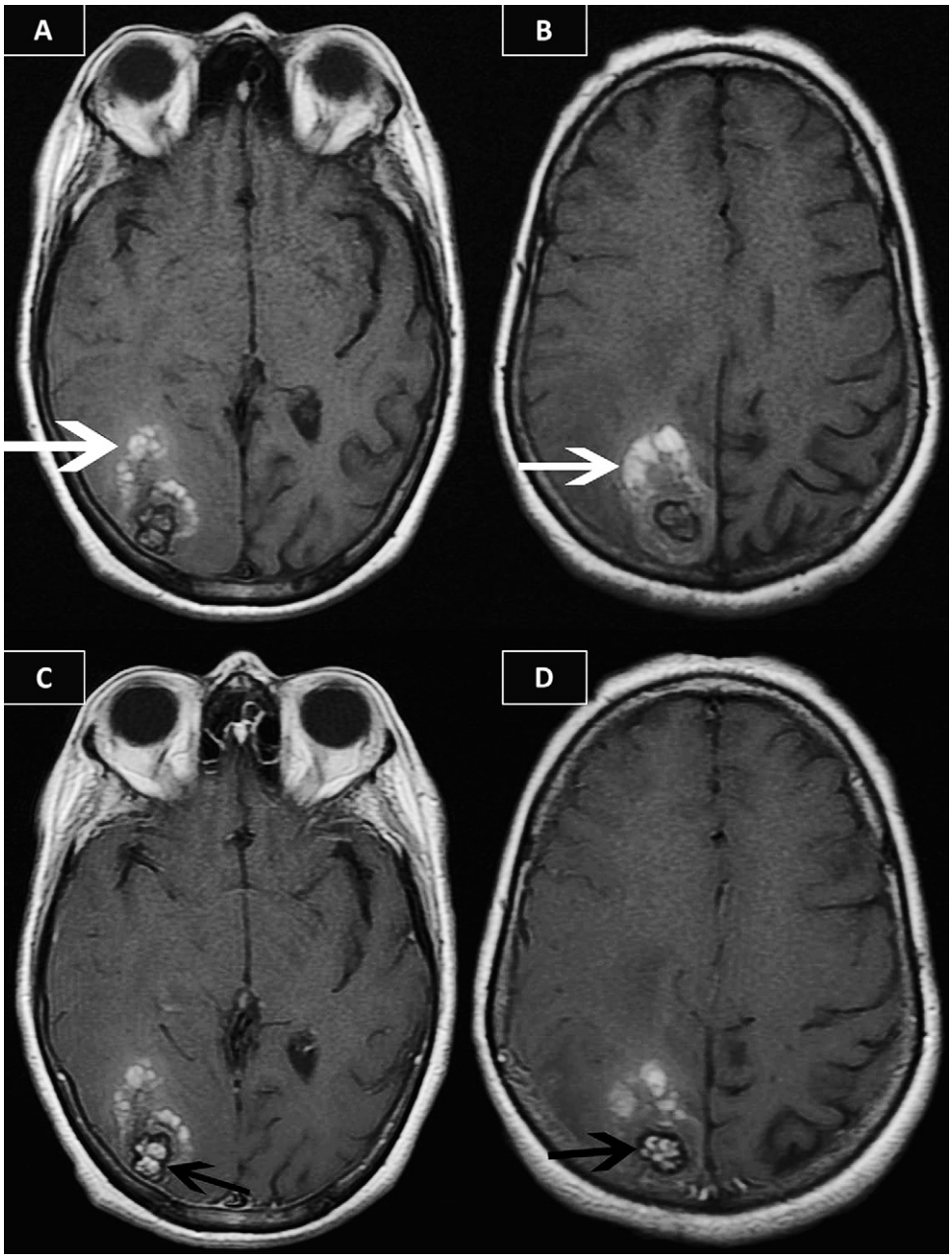

Figure 1 Magnetic resonance imaging of the head. **(A,B)** Axial T1-weighted images show high signal foci in the right occipital area representing hemorrhage *(white arrows)*. **(C,D)** Axial T1-weighted images at same anatomic levels the after intravenous administration of gadolinium contrast demonstrate enhancement in central portions of lesions *(black arrows)*. These findings are consistent with cavernous malformations of the brain.

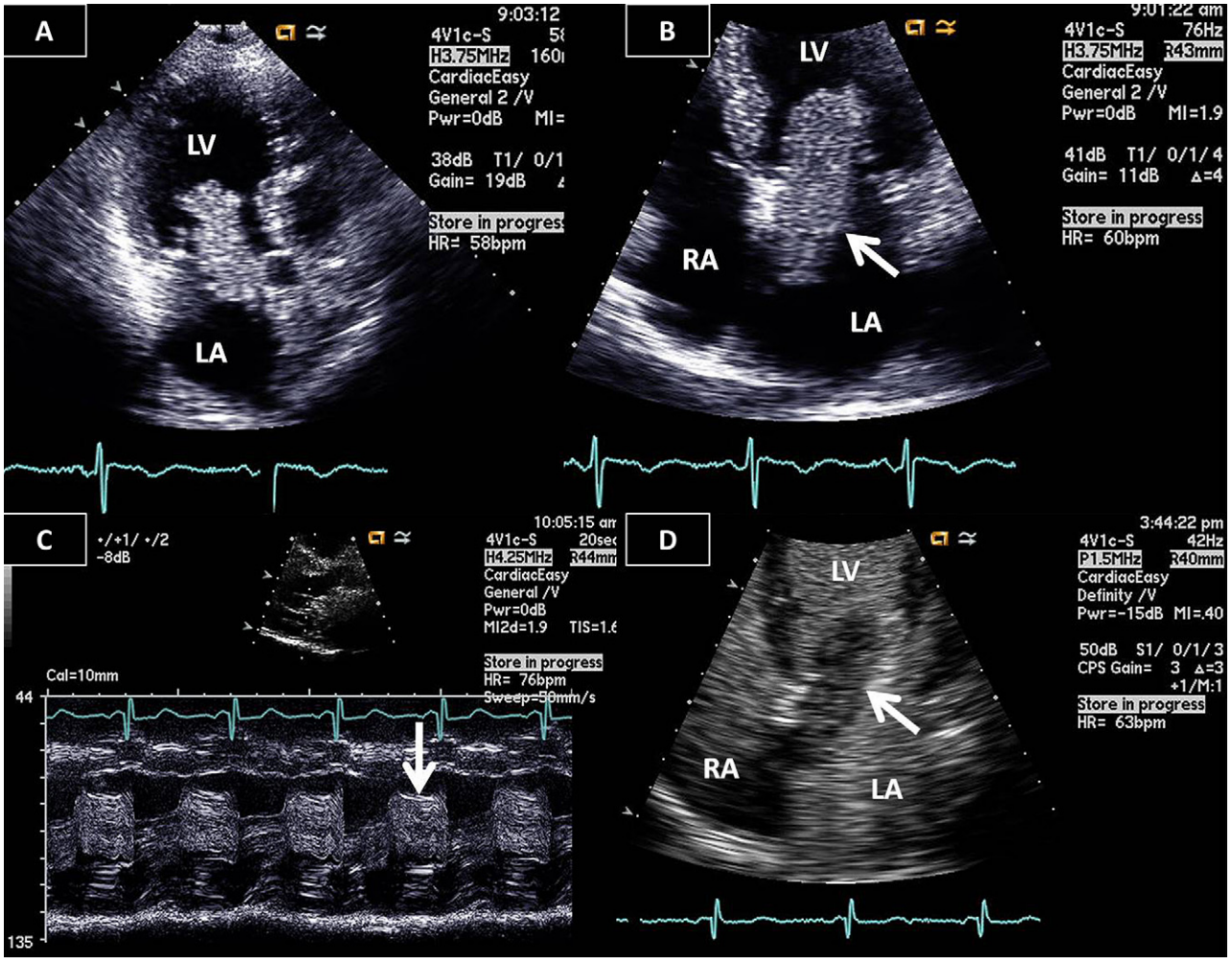

Figure 2 Transthoracic echocardiography. **(A)** Apical three-chamber view and **(B)** apical four-chamber view demonstrate a large myxoma *(arrow)* protruding from the left atrium (LA) across the mitral valve into the left ventricle (LV). **(C)** M-mode recording demonstrates tumor plop during diastole *(arrow)*. **(D)** Heterogeneous uptake of perflutren microbubble contrast by the myxoma *(arrow)*. *RA*, Right atrium.

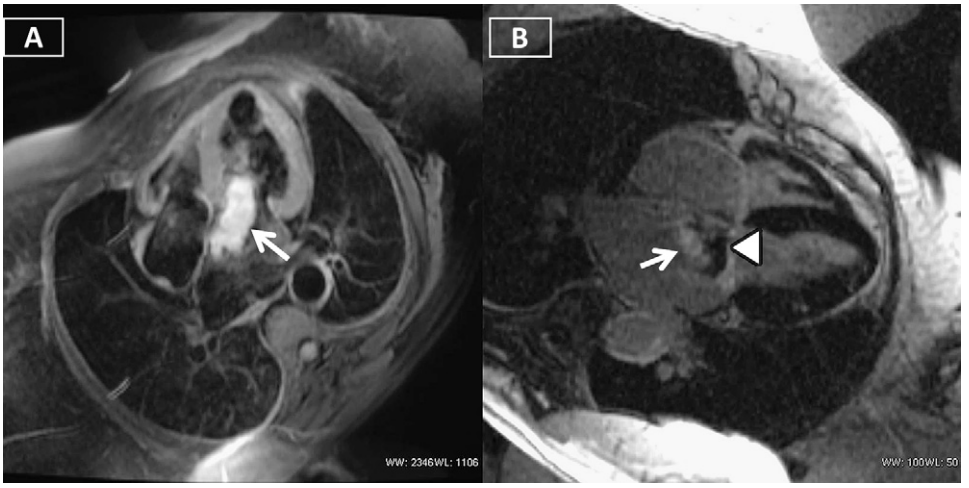

Figure 3 Cardiac magnetic resonance imaging. **(A)** Double inversion recovery fast spin-echo image with fat saturation in the four-chamber view shows high signal mass *(arrow)* in left atrium extending across the mitral valve. **(B)** Contrast-enhanced inversion recovery gradient-echo magnetic resonance image in the four-chamber view shows enhancement of tumor *(arrow)*.

Figure 4 Gross surgical specimen. A red and pink friable myxoma measuring 4.5 × 3.0 × 0.8 cm was excised from the left atrium.

direct tumor embolization or mycotic aneurysms of cerebral vasculature or rupture of mycotic aneurysms of cerebral arteries. Mycotic aneurysms themselves may be a late complication of direct tumor embolization; tumor emboli are believed to release vasoactive substances that weaken the vessel wall and lead to aneurysm formation.[3] However, neurologic deficits in our patient were related to a different mechanism, namely, the presence of multiple bleeding cerebral cavernous malformations (CCMs).

CCMs are hamartous dysplasias characterized by blood cavities bounded by a single layer of endothelium without muscular tissue or intervening brain parenchyma.[4] CCMs may be spread throughout the central nervous system but are predominantly seen in cerebral hemispheres.[5] CCMs often coexist with mesenchymal anomalies in other organs, including the liver, kidneys, and retinas.[6]

CCMs can occur in sporadic form or as a familial autosomal dominant trait with incomplete penetrance and variable expressivity.[7] Three genes have been identified in sporadic and familial forms; CCM1, CCM2, and CCM3 gene mutations are seen in 94% of familial and 57% to 71% of sporadic cases with multiple hemangiomas.[8] The loss-of-function mutations in the zebrafish homologues of CCM1 and CCM2 cause defects of both the heart and the vasculature, suggesting that the coexistence of atrial myxoma and CCM may not be purely coincidental but may be due to a common genetic defect.[9] Patients with cardiac myxoma probably all warrant investigation for central nervous system lesions (not necessarily for CCM but for the more common, and definitely associated, lesions such as aneurysm). To the best of our knowledge, ours is only the second reported case of concomitant occurrence of CCM and atrial myxoma; the first appeared only in 2008.[10]

REFERENCES

1. Goldberg HP, Glenn F, Dotter CT, Steinberg I. Myxoma of the left atrium: Diagnosis made during life with operative and post-mortem findings. Circulation 1952;6:762-7.
2. Markel ML, Waller BF, Armstrong WF. Cardiac myxoma—a review. Medicine 1987;66:114-25.
3. Damasio H, Seabra-Gomes R, da Silva JP, Damasio AR, Antunes JL. Multiple cerebral aneurysm and cardiac myxoma. Arch Neurol 1975;32:269-70.
4. Tagle P, Huete I, Mendez J, Del Vilhar S. Intracranial cavernous angioma: presentation and management. J Neurosurg 1986;64:720-3.
5. Robinson JR, Awad IA, Little JR. Natural history of cavernous angiomas. J Neurosurg 1991;75:709-14.
6. Drigo P, Battistella PA, Mammi I. Familial cerebral, hepatic, and retinal cavernous angiomas. Child Nerv Syst 1995;11:65.
7. Rigamonti D, Hadley MN, Drayer BP, Johnson PC, Hoenig-Rigamonti K, Knight JT, et al. Cerebral cavernous malformations: incidence and familial occurrence. N Engl J Med 1988;319:343-7.
8. Felbor U, Gaetzner S, Verlaan DJ, Vijzelaar R, Rouleau GA, Siegel AM. Large germline deletions and duplication in isolated cerebral cavernous malformation patients. Neurogenetics 2007;8:149-51.
9. Mably JB, Chuang LP, Serluca FC, Mohideen MPK, Chen JN, Fishma MC. Santa and valentine pattern concentric growth of cardiac myocardium in the zebrafish. Development 2006;133:3139-46.
10. Ardeshiri A, Ardeshiri A, Beiras-Fernandez A, Steinlein OK, Winkler PA. Multiple cerebral cavernous malformations associated with extracranial mesenchymal anomalies. Neurosurg Rev 2008;31:11-8.

Video 1 Apical 4-chamber view of a transthoracic echocardiogram shows tumor plop of the left atrial myxoma across the mitral valve during diastole.

Video 2 Transthoracic echocardiogram in the apical 4-chamber view after intravenous injection of perflutren lipid microsphere contrast demonstrates a heterogenous uptake pattern within the left atrial myxoma.

Video 3 Cardiac magnetic resonance imaging in four-chamber view using nonbalanced cine gradient-echo bright blood sequence shows a mass attached to the interatrial septum prolapsing across the mitral valve during diastole typical of left atrial myxoma.